An Osmolyte Effect on the Heat Capacity Change for Protein Folding†

Isabel M. Plaza del Pino and Jose M. Sanchez-Ruiz*

Facultad de Ciencias, Departamento de Quimica-Fisica e Instituto de Biotecnologia, 18071-Granada, Spain

Received February 15, 1995; Revised Manuscript Received April 24, 1995⊗

ABSTRACT: We have carried out a differential scanning calorimetry study into the pH effect on the thermal denaturation of ribonuclease A at several concentrations of the osmolyte sarcosine. In order to properly analyze these data, we have elaborated the thermodynamic theory of the linkage between temperature, cosolvent, and pH effects. The denaturation heat capacity increases with sarcosine concentration. The effects of temperature and sarcosine concentration on the denaturation enthalpy and entropy values are well described by convergence equations, with convergence temperatures of around 100 °C for the enthalpy and around 112 °C for the entropy; we suggest that these effects might be related to a solvent-induced alteration of the apolar-group-hydration contribution to the folding thermodynamics. From our data, we estimate that about 70 extra molecules of water are thermodynamically bound upon ribonuclease denaturation in diluted aqueous solutions of sarcosine; this number is 6−9 times smaller than that predicted on the basis of the following two premises: (a) the osmolyte is strongly excluded from the surface of both the native and the denatured protein and (b) the denatured state is a fully solvated chain. We suggest that at least one of these two premises does not hold. We briefly comment on the potential use of cosolvent effects on thermal denaturation to evaluate the degree of hydration of denatured proteins (thus providing an independent measure of the consequence of their possible residual structure) and, also, on the possibility of finding substances that are more efficient protein stabilizers than known osmolytes are.

Much effort has been devoted in recent years to understanding the factors that determine protein stability and developing approaches that allow researchers to design proteins with enhanced stability. This "protein stability problem" is also confronted by some living organisms which are subjected to denaturing stresses (heat, freezing, high urea concentration, etc.); as a response, these organisms produce relatively low concentrations of certain low molecular weight substances (stabilizing osmolytes) which appear to enhance stability without detrimental effects on biological activity (Yancey et al., 1982; Arakawa & Timasheff, 1985; Timasheff, 1992; Santoro et al., 1992). The main factor responsible for this stabilizing effect was disclosed by Timasheff and co-workers (Arakawa & Timasheff, 1985; Timasheff, 1992) and is related to the fact these osmolytes are preferentially excluded from the protein surface, that is, they cause the preferential hydration of the protein; this effect should favor the protein state with the lower exposed surface, thus displacing the denaturation equilibrium toward the native state and bringing about a higher denaturation temperature in the presence of the osmolyte. In an important paper, Bolen and co-workers (Santoro et al., 1992) showed that the stabilizing effect of osmolytes may extend well beyond their physiological concentration range; thus, several-molar concentrations of glycine-based osmolytes were found to produce very large increments (up to about 20 °C) in the denaturation temperature of model globular proteins.

However, one potentially interesting aspect of osmolyte action has received little attention; namely, the possible osmolyte effect on the heat capacity change for protein denaturation. The interest of characterizing this (possible) effect is suggested by the two following facts: (1) the thermodynamic stability of proteins is best described in terms of the denaturation Gibbs energy *versus* temperature profile (the protein stability curve), the shape of which depends on the value of the denaturational heat capacity change (Becktel & Schellmann, 1987; Sanchez-Ruiz, 1995), and (2) Recent work shows that the denaturational heat capacity change may be directly interpreted in molecular terms as mainly reflecting the interactions with the solvent of the polar and apolar groups which are exposed upon denaturation (Murphy & Gill, 1991; Makhatadze & Privalov, 1990; Privalov & Makhatadze, 1990, 1992; Spolar et al., 1992; Murphy et al., 1992; Sanchez-Ruiz, 1995).

Here we present a differential scanning calorimetry (DSC)[1] study primarily addressed to determine the effect of the osmolyte sarcosine on the heat capacity change for the denaturation of a model protein, ribonuclease A (RNase A). In fact, Santoro et al. (1992) reported DSC data on this system but only at a single pH (= 6). Accordingly, we aimed at a full characterization of the pH dependence of the thermodynamic parameters for RNase A denaturation within the acidic pH range and for several water−sarcosine mixtures, which (assuming that the denaturation enthalpy does not depend explicitly on pH) will allow us to obtain reliable estimates of the denaturational heat capacity changes from the temperature dependence of the denaturation enthalpy values.

Proper analysis of our denaturation data requires the use of the thermodynamic theory of the linkage between temperature, pH, and cosolvent effects, which is summarized in the Basic Theory section of this paper. This theoretical framework, together with our experimental denaturation data,

† This research was supported by Grant PB93-1087 from the DGICYT (Spanish Ministry of Education and Science).
⊗ Abstract published in *Advance ACS Abstracts,* June 15, 1995.

[1] Abbreviations: ASA, water-accessible surface area; DSC, differential scanning calorimetry; RNase, ribonuclease.

0006-2960/95/0434-8621$09.00/0

enables us to obtain the denaturational changes in Gibbs energy, number of protons bound, protein−sarcosine preferential interaction, and protein preferential hydration as a function, in principle, of pH, temperature, and cosolvent (sarcosine) concentration.

Clearly, the general approach employed in this work is that of classical thermodynamics, which only provides phenomenological interconnections between thermodynamic magnitudes. Nevertheless, we shall deviate from this purely phenomenological approach when discussing two rather surprising results: (1) the denaturation heat capacity change increases with sarcosine concentration, and concomitantly, the denaturation enthalpy and entropy values also increase (at a given temperature) in such a way that convergence behavior is observed, with convergence temperatures around 100 °C for the enthalpy and around 112 °C for the entropy; and (2) the calculated value of the denaturational change in preferential hydration indicates that about 70 molecules of water become thermodynamically bound upon RNase denaturation in diluted sarcosine solutions, a number which is 6−9 times smaller than the value calculated by assuming that (a) sarcosine is preferentially excluded from the surface of both the denatured and the native states and (b) the denatured state behaves as a fully-solvated chain.

EXPERIMENTAL PROCEDURES

Bovine pancreatic RNase A (Type XII-A, lot 61H7185) and sarcosine were purchased from Sigma Chemical Co. and used without further purification. Degassed and deionized water was used throughout. Ribonuclease solutions in sarcosine−water (concentration about 2 mg/mL) were prepared by dilution of a stock solution which had been exhaustively dialyzed against an aqueous buffer. DSC experiments were carried out in sarcosine−water mixtures of the followings sarcosine molarities (moles of sarcosine per liter of solution): 0, 1.5, 3, 4.5, 6, and 7.8 M. Density measurements allowed us to express these concentrations in terms of sarcosine molality (moles of sarcosine per kilogram of water): 0, 1.44, 2.79, 4.06, 5.27, and 6.61 m, respectively. At each of these sarcosine concentrations, several DSC experiments (see below for details) within the approximate pH range 3−6 were carried out. Sarcosine has a protonation with a pK value around 2 (Christensen et al., 1976) which, at the high concentrations used, provides significant buffering capacity, even in the pH range 3−6. Nevertheless, we included 25 mM glycine in all the sarcosine−water mixtures for consistency with previously published DSC work on RNase denaturation in water, which has typically employed this buffer. However, when we tried to carry out control DSC experiments in water, we found that, as was to be expected, 25 mM glycine does not provide adequate buffering capacity above pH about 4 and we decided to employ 50 mM potassium acetate instead. In order to ensure that this buffer change (from acetate in water to glycine in water−sarcosine) does not introduce a spurious alteration in the data, we performed several DSC experiments in sarcosine−water mixtures of sarcosine concentrations 3 and 6 M and using 50 mM acetate as buffer. We found no significant difference between the results of these experiments and the results of those previously carried out at the same sarcosine concentrations but using 25 mM glycine as buffer.

Calorimetric experiments were carried out in a differential scanning calorimeter DASM-1 described by Privalov et al. (1975), which cell volumes of 1 mL, under an extrapressure of 1 atm to avoid any degassing during the heating. The nominal scanning rate was 1 K/min; actually, the scanning rate increased somewhat with the sarcosine content in the solvent (from 0.98 K/min in water to 1.16 K/min in 7.8 M sarcosine), probably due to the smaller total heat capacity of the concentrated sarcosine solutions.

A single transition was always observed in the DSC thermograms, except at the higher sarcosine concentration employed (7.8 M or 6.61 m) and pH < 4, where a broad and weak transition was progressively evident (as the pH was lowered) on the high-temperature side of the major one (results not shown). Since we do not know the origin of this weak transition, these thermograms are not included in the global analysis described under Results and Discussion (we note, nevertheless, that the parameters of the major transition fit the general trends suggested by the rest of the data).

DSC scans were terminated several degrees above the end of the calorimetric transition, to ensure that the posttransition heat capacity levels were adequately defined. Second (reheating) scans were always performed after cooling from the first ones; in all cases, denaturation was found to be highly reversible (80−90% reversibility, calculated as the ratio of the areas of the second to the first transition).

As is often the case with DSC thermograms for protein denaturation [see, for instance, Brandts and Lin (1990)], we found that after correcting for the instrumental (solvent−solvent) baseline, the pre- and posttransition heat capacity levels showed linear dependencies with temperature but with clearly different slopes in many cases. Hence, the value for the denaturation heat capacity calculated from the linear extrapolation of these levels would display a significant temperature dependence [larger, in fact, than that expected from the accurate DSC measurements of the heat capacity of the denatured state reported by Privalov and Makhatadze (1990)]; in some cases the calculated heat capacity change would even appear to change sign within the temperature range of the calorimetric transitions [a similar problem was described by Brandts and Lin (1990)]. We strongly suspect that since the DSC transitions are highly but not completely reversible, the posttransition level is distorted by the occurrence of an irreversible processes (such as aggregation, which is expected to be an endothermic process). Of course, this problem makes very unreliable the calculation of the heat capacity change from the pre- and posttransition levels (in any case, the values calculated in this way showed a large scatter); however, it should not affect significantly the denaturational enthalpy values derived from the transitions after these levels were connected by a suitable chemical baseline, as is described below.

The DSC transitions were corrected for the effect of the instrument time response as previously described (Galisteo et al., 1991) and the pre- and posttransition levels were connected by a cubic splines function (see Figure 1A). The resulting excess heat capacity *versus* temperature profiles were fitted with the following two-state equation:

$$C_p^{ex} = \frac{\Delta_N^D H_m \Delta H^{vH}}{RT^2} \frac{K}{(1+K)^2} \qquad (1)$$

where $\Delta_N^D H_m$ is the denaturation enthalpy (*i.e.*, the calori-

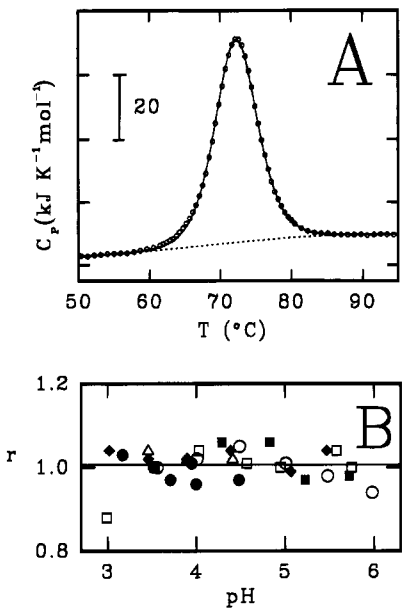

FIGURE 1: (A) DSC thermogram corresponding to the thermal denaturation of RNase in 4.5 M sarcosine, pH = 4.39. (○) Experimental heat capacity data corrected for the instrumental baseline and the time response of the calorimeter. (- - -) Chemical baseline obtained by connecting the pre- and posttransition levels with a cubic splines function. (—) Best fit of eq 1 to the excess heat capacity profile. (B) Calorimetric to van't Hoff enthalpy ratio for the thermal denaturation of RNase at several pH values and the following sarcosine concentrations: (○) 0 m, (△) 1.44 m, (●) 2.79 m, (♦) 4.06 m, (□) 5.27 m, and (■) 6.61 m.

metric enthalpy) and ΔH^{vH} is the so-called van't Hoff enthalpy, which gives the temperature dependence of the denaturation equilibrium constant (K):

$$K = \exp[-(\Delta H^{vH}/R)(1/T - 1/T_m)] \quad (2)$$

where the denaturation temperature, T_m, is defined as the temperature at which $K = 1$. Equations 1 and 2 assume that the temperature dependency of the enthalpies may be neglected within the comparatively narrow range of a given calorimetric transition, and the subscript m attached to the calorimetric enthalpy means that its value is to be assigned to the denaturation temperature. The fits of eqs 1 and 2 to the experimental data were always excellent (see, for instance, Figure 1A) and the calorimetric enthalpies derived from them were essentially identical to those calculated from the area under the transitions. These fittings also provide a stringent two-state test, since the van't Hoff enthalpy was an independent fitting parameter and $\Delta H^{vH} = \Delta_N^D H_m$ was *not* assumed; in fact, we found that the calorimetric to van't Hoff enthalpy ratio never deviated significantly from unity (Figure 1B), thus demonstrating close adherence to the two-state equilibrium model.

BASIC THEORY

We briefly summarize here some thermodynamic definitions and results which will prove essential in the subsequent analysis and discussion of our calorimetric data. The supporting information provides mathematical derivations of the equations given below and further details regarding the thermodynamic linkage between temperature, cosolvent, and pH effects.

We employ the convention of Scatchard (1946) and use subscripts 1, 2, and 3 to designate the "main" solvent (water), the protein, and the cosolvent (sarcosine), respectively; thus, m_3 is the cosolvent molality (moles of sarcosine per kilogram of water). ν stands for the number of moles of protons stoichiometrically bound to a mole of protein. Following Timasheff (1993), we define the protein–cosolvent preferential interaction parameter (ϕ_{23}) as a measure of the mutual perturbation of the chemical potentials of protein and cosolvent: $\phi_{23} = (\partial\mu_2/\partial m_3)_{T,pH,m_2} = (\partial\mu_3/\partial m_2)_{T,pH,m_3}$.

Denaturational changes of thermodynamic quantities are labeled with the symbol Δ_N^D. The denaturational Gibbs energy change is the difference between the standard chemical potentials of the denatured and native protein ($\Delta_N^D G = \mu_2^D - \mu_2^N$) and is to be considered a function of temperature, pH, and cosolvent (sarcosine) concentration. The first derivatives of $\Delta_N^D G$ are easily related [see, for instance, Alberty (1969)] with the denaturational changes in entropy, proton binding, and preferential interaction parameter ($\Delta_N^D\phi_{23} = \phi_{23}^D - \phi_{23}^N$):

$$\left(\frac{\partial\Delta_N^D G}{\partial T}\right)_{pH,m_3} = -\Delta_N^D S \quad (3)$$

$$\left(\frac{\partial\Delta_N^D G}{\partial pH}\right)_{T,m_3} = (\ln 10)RT\Delta_N^D\nu \quad (4)$$

$$\left(\frac{\partial\Delta_N^D G}{\partial m_3}\right)_{T,pH} = \Delta_N^D\phi_{23} \quad (5)$$

The denaturational changes in proton binding and preferential interaction parameter may also be expressed in terms of the pH and cosolvent effects on the denaturation temperature:

$$\Delta_N^D\nu = \Delta_N^D H_m[(\ln 10)\cdot RT_m^2\cdot(\partial pH/\partial T_m)_{m_3}]^{-1} \quad (6)$$

$$\Delta_N^D\phi_{23} = \frac{\Delta_N^D H_m}{T_m}\left(\frac{\partial T_m}{\partial m_3}\right)_{pH} \quad (7)$$

Several linkage relationships are obtained from equalities between second derivatives of the denaturational Gibbs energy change. We will make direct use of the two following ones:

$$\left(\frac{\partial\Delta_N^D S}{\partial m_3}\right)_{T,pH} = -\left(\frac{\partial\Delta_N^D\phi_{23}}{\partial T}\right)_{pH,m_3} \quad (8)$$

$$\left(\frac{\partial\Delta_N^D H}{\partial pH}\right)_{T,m_3} = -(\ln 10)RT^2\left(\frac{\partial\Delta_N^D\nu}{\partial T}\right)_{pH,m_3} \quad (9)$$

We define (Timasheff, 1993) the preferential hydration of the protein (Γ_{21}) as the amount of water that must be added (or removed) upon protein addition to the system in order to maintain constant the water chemical potential. The denaturational changes in preferential hydration ($\Delta_N^D\Gamma_{21} = \Gamma_{21}^D - \Gamma_{21}^N$) and protein–cosolvent preferential interaction ($\Delta_N^D\phi_{23}$) may be related by

$$\Delta_N^D\Gamma_{21} = \frac{\Delta_N^D\phi_{23}}{\bar{V}_1\cdot(\partial\Pi/\partial m_3)_T} \quad (10)$$

where $\bar{V}_1$ is the molar volume of water and Π is the osmotic pressure of the water–cosolvent mixture (with the cosolvent as a nondiffusible component and water as the diffusible one). Since $\Delta_N^D\phi_{23} = \partial\Delta_N^DG/\partial m_3$ (eq 5), $\Delta_N^DG = -RT \ln K$ and $\Pi\bar{V}_1 = -RT \ln a_1$, eq 10 may also be written as $\Delta_N^D\Gamma_{21} = (\partial \ln K/\partial \ln a_1)_{T,pH}$, which shows that application of eq 10 is equivalent to the calculation of the denaturational change in preferential hydration from the slope of a Wyman plot (ln K *versus* logarithm of water activity: Wyman, 1964).

Strictly, all denaturational changes of thermodynamic quantities depend on temperature, pH, and cosolvent concentration. However, we will assume in our subsequent analysis of RNase A denaturation in sarcosine–water that the T and m_3 dependencies of the denaturational change in proton binding may be neglected, at least as a first approximation; thus, $\Delta_N^D\nu$ will be considered as function of pH exclusively (this assumption will be justified later in this paper). This $\Delta_N^D\nu = f(\text{pH})$ approximation implies that the denaturational changes in enthalpy, preferential interaction parameter, and heat capacity depend on cosolvent concentration and temperature *but not on pH*.

Accurate DSC measurements over a broad temperature range (Privalov & Gill, 1988; Privalov et al., 1989; Privalov & Makhatadze, 1990, 1992) indicate that heat capacity changes for globular protein denaturation usually do depend somewhat on temperature, decreasing at high temperature and apparently extrapolating to zero at temperatures well above 100 °C. Nevertheless, it appears that no serious error is introduced if $\Delta_N^DC_p$ is taken as a constant within the temperature range from about 20 °C to about 80 °C (Privalov & Gill, 1988; Privalov, 1989); in addition, the comparatively narrow range of T_m values, together with the experimental uncertainties of the $\Delta_N^DH_m$ values, makes it very unlikely that the small T dependence of $\Delta_N^DC_p$ could be detected in a $\Delta_N^DH_m$ *versus* T_m plot. Accordingly, we will employ the temperature-independent heat capacity approximation and further assume that $\Delta_N^DC_p$ is a function of cosolvent concentration exclusively. Hence, the slope of a plot of $\Delta_N^DH_m$ *versus* T_m for a given m_3 value will be taken as the denaturational heat capacity change corresponding to that cosolvent concentration.

Unlike Δ_N^DH, $\Delta_N^D\phi_{23}$, and $\Delta_N^DC_p$, the denaturational entropy change depends on pH, even under the $\Delta_N^D\nu = f(\text{pH})$ approximation. Therefore, prior to the analysis of their temperature dependence, denaturation entropies must be corrected to a common pH value (pH°). This can be accomplished by using the following equation:

$$\Delta_N^DS_m^\circ = \Delta_N^DS_m - (\ln 10)R\int_{pH_m}^{pH^\circ}\Delta_N^D\nu \, d\text{pH} \qquad (11)$$

where $\Delta_N^DS_m$ (calculated as $\Delta_N^DH_m/T_m$) is assigned to the denaturation temperature (T_m) corresponding to a given pH value (pH_m) and $\Delta_N^DS_m^\circ$ stands for the denaturation entropy at the same temperature but at a different pH value (pH° $\neq$ pH_m).

RESULTS AND DISCUSSION

Effect of pH and Sarcosine Concentration on the Denaturation Temperature. Figure 2A shows the T_m *versus* pH profiles corresponding to RNase denaturation in water and in the five water–sarcosine mixtures studied in this work. It is clear that the denaturation temperature increases with sarcosine concentration within the studied pH range.

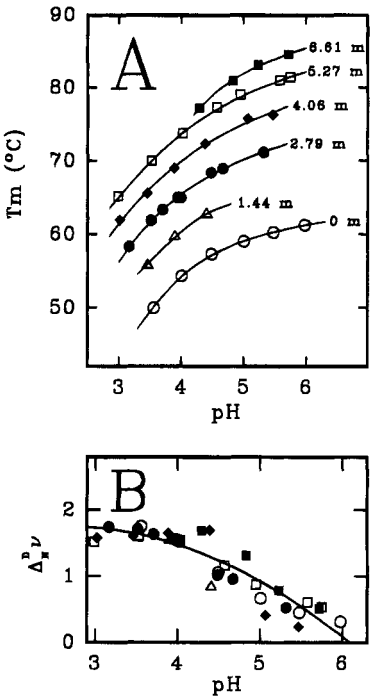

FIGURE 2: (A) Denaturation temperature of RNase as a function of pH for several sarcosine concentrations. The lines are the best fits of eq 12 to the experimental T_m data. (B) pH dependence of the number of moles of protons taken from the solvent upon denaturation of a mole of protein; the symbols refer to the sarcosine concentration and have the same meaning as in Figure 1B. The line is shown to guide the eye and has no theoretical significance.

An analytical representation of the T_m/pH profiles is useful for interpolation and derivation purposes. In fact, we found it more convenient to fit pH as a function of T_m, according to the following empirical equation:

$$\text{pH} = a + bT_m + c\exp(dT_m) \qquad (12)$$

As shown in Figure 2A, eq 12, together with the optimum values of the constants $\{a, b, c, d\}$ for each solvent mixture, describes very accurately the experimental {pH, T_m} data.

The denaturational change in proton binding at the denaturation temperature corresponding to given solvent conditions (pH and m_3) may be obtained from the derivative $\partial\text{pH}/\partial T_m$ evaluated from eq 12 and the denaturational enthalpy change ($\Delta_N^DH_m$) by using eq 6. Values of $\Delta_N^D\nu$ corresponding to different {pH, m_3, T_m} conditions are plotted *versus* pH in Figure 2B. Within experimental uncertainty, they seem to define a common pH dependence, which supports the $\Delta_N^D\nu = f(\text{pH})$ approximation.

Effect of Temperature and Sarcosine Concentration on the Denaturational Enthalpy Change. According to the $\Delta_N^D\nu = f(\text{pH})$ approximation, the denaturation enthalpy at the denaturation temperature ($\Delta_N^DH_m$) is to be considered a function of the T_m value and the cosolvent concentration. We have found that these functional dependencies may be accurately described on the following basis: (1) the denaturational heat capacity change increases with cosolvent molality, m_3, and (2) the $\Delta_N^DH_m$ *versus* T_m dependencies show convergence behavior.

By "convergence behavior" we mean that the denaturation enthalpies would attain a common value ($\Delta_N^D H^*$) when extrapolated to a given hypothetical temperature (T_H^*) under the temperature-independent heat capacity approximation:

$$\Delta_N^D H_m = \Delta_N^D H^* + \Delta_N^D C_p(m_3)[T_m - T_H^*] \qquad (13)$$

Equation 13 was fitted to our entire $\Delta_N^D H_m/T_m$ set by nonlinear least-squares procedures. Fitting parameters were the several denaturation heat capacity changes corresponding to the water–sarcosine mixtures under analysis [$\Delta_N^D C_p$ in water ($m_3 = 0$) was kept fixed at the (very accurately known) experimental value at 50 °C, 5.3 kJ·K^{-1}·mol^{-1}; Makhatadze & Privalov, 1995], as well as the common convergence parameters ($\Delta_N^D H^*$ and T_H^*), which are assumed not to depend on solvent composition. The fit was excellent[2] (see Figure 3A) with a standard deviation of 12 kJ/mol, which is about the experimental uncertainty of the denaturation enthalpy values. The optimum values obtained for the fitting parameters are given in Table 1 (convergence parameters) and Figure 4 (heat capacity changes).

The above calculations assume that the denaturation enthalpy does not depend explicitly on pH. This should be an excellent approximation, since ionization enthalpies are expected to be very small (in particular in the acidic pH range, where the protein–solvent proton exchange is dominated by carboxylic acid ionization). In addition, the approximation is supported by the fact that $\Delta_N^D \nu$ does not appear to depend on temperature (Figure 2B and eq 9).

Effect of Temperature and Sarcosine Concentration on the Denaturational Entropy Change. Denaturation entropy depends on pH, even under the $\Delta_N^D \nu = f(\text{pH})$ approximation. Therefore, denaturation entropies ($\Delta_N^D S_m = \Delta_N^D H_m/T_m$) were corrected to a common pH value (pH° = 4.5) by using the $\Delta_N^D \nu$ values previously determined (Figure 2B) and eq 11. Again, the temperature and cosolvent concentration dependencies of the $\Delta_N^D S_m^\circ$ values thus obtained may be accurately described on the basis of (1) the increase in $\Delta_N^D C_p$ upon increasing sarcosine concentration (Figure 4) and (2) the convergence behavior, which in this case is formulated as

$$\Delta_N^D S_m^\circ = \Delta_N^D S^* + \Delta_N^D C_p(m_3) \ln (T_m/T_S^*) \qquad (14)$$

where T_S^* is the hypothetical temperature at which the denaturation entropies would reach a common value ($\Delta_N^D S^*$) under the temperature-independent heat capacity extrapolation.

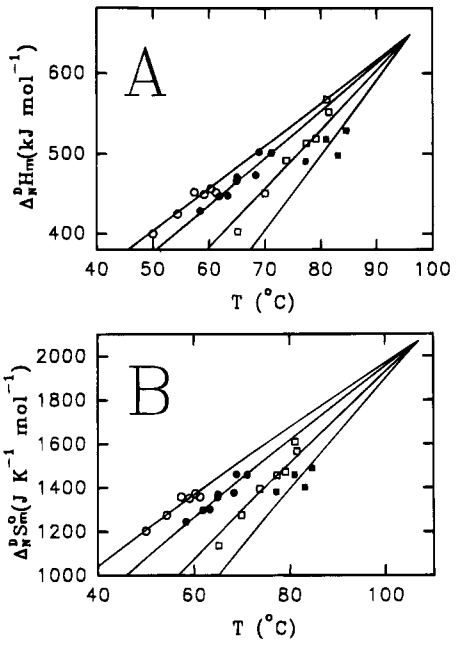

FIGURE 3: Plots of denaturation enthalpy (A) and denaturation entropy (B) *versus* temperature for the thermal denaturation of RNase in water–sarcosine mixtures of the following sarcosine concentrations: (○) 0 m, (●) 2.79 m, (□) 5.27 m, and (■) 6.61 m. For the sake of clarity, we have omitted the data corresponding to sarcosine concentrations 1.44 and 4.06 m. The lines are the dependencies predicted by the convergence equations 13 (A) and 14 (B), together with the convergence parameters given in Table 1 and the denaturation heat capacity values shown in Figure 4. Note that the lines in panel B are not straight lines but show curvature, as predicted by eq 14.

Table 1: Convergence Parameters

	RNase denaturation in water–sarcosine[a]	cytochrome *c* denaturation in water–methanol[b]	apolar gas dissolution[c]
T_H^* (°C)	96 (92–103)[d]	101.9 ± 2	91.8 ± 7.7
$\Delta_N^D H^*$ (kJ/mol)	648 (623–685)[d]	564 ± 21	
	[5.23][e]	[5.42][e]	
T_S^* (°C)	107 (99–125)[d]	111.9 ± 2	111.6 ± 5.3
$\Delta_N^D S^*$	2.07 (1.95–2.32)[d]	1.63 ± 0.01	
(kJ·K^{-1}·mol^{-1})	[1.67 × 10^{-2}][e]	[1.57 × 10^{-2}][e]	

[a] This work. [b] Values taken from Fu and Freire (1992). [c] Calculated from the data for rare gases and alkanes given by Privalov and Gill (1988). [d] Standard uncertainty intervals calculated by using the method proposed by Bevington (1969). Bevington intervals take into account the effect of correlations between *all* fitting parameters and are not constrained to be symmetric around the best value; therefore, they cannot be given as ± uncertainty, but each interval must be specified by giving its two extreme values. [e] Convergence entropy and enthalpy values normalized per mole of residues; the number of residues of RNase and cytochrome *c* are 124 and 104, respectively.

The fit of eq 14 to our entire $\Delta_N^D S_m^\circ/T_m$ set was excellent[2] (Figure 3B) and the optimum values for the fitting parameters (the several denaturational heat capacity changes and the common convergence parameters, $\Delta_N^D S^*$ and T_S^*) are given in Figure 4 and Table 1. Note that the $\Delta_N^D C_p(m_3)$ dependence obtained from this analysis is essentially identical to that previously derived from the denaturation enthalpies

[2] The text describes global analysis of the enthalpy (eq 13 and Figure 3A) and entropy (eq 14 and Figure 3B) data, which is similar to that previously employed by Fu and Freire (1992). However, the increase in denaturation heat capacity and the convergence behavior are already evident from the enthalpy and entropy data, even if such global analysis is not carried out. Thus, independent analysis of the linear temperature dependencies of the denaturation enthalpies yields the following denaturation heat capacity values (kilojoules per kelvin per mole): 5.0 ± 0.8 ($m_3 = 0$), 6.0 ± 0.8 ($m_3 = 2.79$), 6.7 ± 0.9 ($m_3 = 4.06$), and 8.8 ± 0.5 ($m_3 = 5.27$). Essentially identical values were derived from the independent analysis of the $\Delta_N^D S$ *versus* ln T dependencies. Plots of denaturation enthalpy or denaturation entropy at a given temperature (interpolated from the corresponding linear temperature dependencies) *versus* $\Delta_N^D C_p$ produce straight lines (as predicted by the convergence equations 13 and 14), the slopes of which yield estimates of the convergence temperature values (T_H^* around 85 °C and T_S^* around 92 °C) in acceptable agreement with the values derived from the global analysis (Table 1).

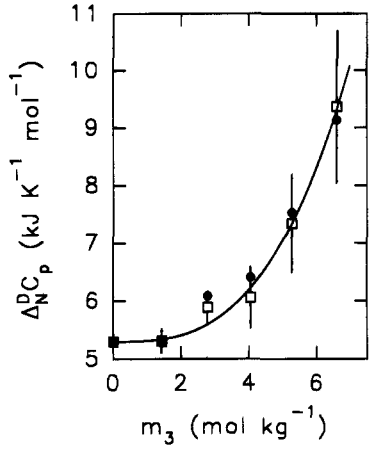

FIGURE 4: Heat capacity change for RNase denaturation as a function of the sarcosine concentration. (□) Values determined from the global fitting of eq 13 to the denaturation enthalpy data (see Figure 3A); the bars represent the standard uncertainty intervals derived from the global fitting. (●) Values determined from the global fitting of eq 14 to the denaturation entropy data. (—) Dependence given by eq 15.

(Figure 4) and both sets of $\Delta_N^D C_p$ data are adequately represented by the following empirical equation:

$$\Delta_N^D C_p = 5.30 + (1.39 \times 10^{-2})(m_3)^3 \qquad (15)$$

where $\Delta_N^D C_p$ has the units kilojoules per kelvin per mole.

Some Comments on the Sarcosine Effect on the Denaturational Heat Capacity Change and the Convergence Behavior. It was often assumed in the past that the large and positive $\Delta_N^D C_p$ values found for protein denaturation were largely due to the exposure to the solvent of apolar groups previously buried in the native structure. More recent work (Murphy & Gill, 1990, 1991; Makhatadze & Privalov, 1990; Spolar et al., 1992; Privalov & Makhatadze, 1992; Murphy et al., 1992) has shown that the large contribution arising from the exposure of apolar groups is expected to be partially offset by a negative contribution that arises from the exposure of polar groups. The simplest formulation of this viewpoint is (Murphy et al., 1992; Sanchez-Ruiz, 1995)

$$\Delta_N^D C_p = \Delta\bar{C}_{ap}\Delta_N^D ASA_{ap} + \Delta\bar{C}_{pol}\Delta_N^D ASA_{pol} \qquad (16)$$

where $\Delta_N^D ASA_{ap}$ and $\Delta_N^D ASA_{pol}$ are the denaturational changes in apolar (ap) and polar (pol) accessible surface area and $\Delta\bar{C}_{ap}$ and $\Delta\bar{C}_{pol}$ stand for the heat capacity changes associated with the exposure of 1 mol·Å^2 of apolar and polar ASA, respectively.

Unfortunately, eq 16 alone does not lead to an unambiguous interpretation of the sharp increase in $\Delta_N^D C_p$ for RNase that is observed at the higher sarcosine concentrations (Figure 4); this is so because the polar and apolar contributions have different sign in water [$\Delta\bar{C}_{ap} > 0$ and $\Delta\bar{C}_{pol} < 0$; see Murphy et al. (1992) and Sanchez-Ruiz (1995)], and the four parameters in eq 16 might change with sarcosine concentration in an *a priori* unknown manner. Thus, not only may the $\Delta\bar{C}_{ap}$ and $\Delta\bar{C}_{pol}$ values be expected to depend on solvent composition but, in addition, the denaturational changes in polar and apolar ASA might also change if, for instance, high sarcosine concentrations alter (or induce) the possible residual structure of the denatured state.

In spite of the above, some insight into the origin of the $\Delta_N^D C_p$ increase is derived from the fact that the denaturation enthalpy and entropy values also change with sarcosine concentration as described by convergence equations (eqs 13 and 14). This type of behavior (with specific denaturational changes) was first described for a set of globular proteins (Privalov & Khechinashvili, 1974; Privalov, 1979; Murphy et al., 1990), although it is less clearly observed with the current data set, as recently compiled by Makhatadze and Privalov (1995). More relevant in relation to our results is the fact that the description of solvent effects in terms of convergence behavior has a precedent. Fu and Freire (1992) reported that the effect of methanol concentration on the enthalpy, entropy, and heat capacity changes for cytochrome *c* denaturation in water−methanol mixtures (0−10% v/v) conform to the convergence equations (eqs 13 and 14 in the present paper); in fact, the global analysis we have carried out follows closely that proposed by these authors. Some differences, however, are noteworthy: $\Delta_N^D C_p$ for cytochrome *c* decreases with methanol concentration in a linear fashion, while $\Delta_N^D C_p$ for RNase A increases with sarcosine concentration as empirically described by a cubic equation (eq 15). On the other hand, there is a remarkable agreement between the convergence temperatures values (T_H^* about 100 °C and T_S^* about 112 °C) found in both cases (see Table 1). Furthermore, and most important (as will be made clear further below), these values also agree with those determined from the analysis of the thermodynamic data for the dissolution of apolar gases in water.

Convergence behavior has been rationalized in molecular terms on the basis of the interactions with solvent of the polar and apolar groups (Murphy & Gill, 1991; Lee, 1991; Murphy et al., 1992; Sanchez-Ruiz, 1995). Also, the relation between the convergence temperatures, T_H^* and T_S^*, for protein folding has been discussed by Baldwin and Muller (1992) and Doig and Williams (1992). More recently, Makhatadze and Privalov (1993, 1995; Privalov & Makhatadze, 1993) have carried out a dissection of protein folding thermodynamics into contributions arising from hydration of polar and apolar groups, configurational entropy, hydrogen bonding, and van der Waals interactions of the buried apolar groups. These authors model the hydration contributions on the basis of gas dissolution data. Therefore, the agreement between the convergence temperature values shown in Table 1 suggest that the effect of some cosolvents (such as sarcosine and methanol) on the denaturational heat capacity, enthalpy, and entropy changes is related to a specific alteration of the apolar group hydration contribution in the Makhatadze−Privalov dissection. We do recognize, nevertheless, that the particular molecular mechanisms involved in such solvent-induced alteration remain obscure to us.

Effect of Temperature and Sarcosine Concentration on the Denaturational Gibbs Energy Change. We consider now the calculation of the denaturational Gibbs energy change, $\Delta_N^D G$, for a given sarcosine concentration (among those experimentally studied) and any arbitrary pH and temperature conditions. This can be accomplished by using the following procedure: (1) the T_m value for the desired m_3 and pH conditions is interpolated by numerically solving eq 12 with the values of the parameters {*a*, *b*, *c*, *d*} previously determined for the given sarcosine concentration; (2) the $\Delta_N^D C_p$ value at that sarcosine concentration is taken as that

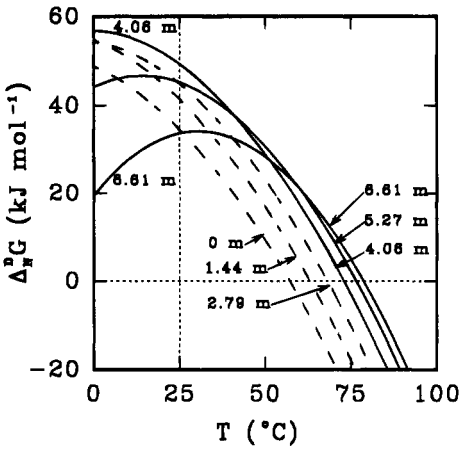

FIGURE 5: Gibbs energy change for RNase denaturation at pH° = 4.5 as a function of temperature and sarcosine concentration. The lines are the protein stability curves ($\Delta_N^D G$ *versus* T profiles) corresponding to the sarcosine molalities shown in the figure.

calculated from the global fitting of eq 13 to the denaturational enthalpy data (Figures 3A and 4); (3) the $\Delta_N^D H$ value at m_3 and T_m ($\Delta_N^D H_m$) is obtained from the convergence equation (eq 13), the $\Delta_N^D C_p$ and T_m values, and the convergence parameters (Table 1); and (4) finally, $\Delta_N^D G$ at {T, pH, m_3} conditions (where $T \neq T_m$) is calculated from the integrated Gibbs–Helmholtz equation:

$$\Delta_N^D G = \Delta_N^D H_m(1 - T/T_m) + \Delta_N^D C_p[T - T_m - T \ln (T/T_m)] \quad (17)$$

We have used the above procedure to obtain the $\Delta_N^D G$ *versus* T profiles (protein stability curves) for several sarcosine molalities and pH° = 4.5, which are shown in Figure 5. Profiles corresponding to other pH values are similar to those shown in that figure but are shifted as prescribed by eq 4 and the $\Delta_N^D \nu$ values.

At this point, we must note that, in this case, there appears to be no correlation between thermodynamic stability, conventionally defined as the denaturation Gibbs energy change at 25 °C, and the "operational stability", as characterized by the denaturation temperature. Thus, T_m increases monotonically with sarcosine concentration, while $\Delta_N^D G$ at 25 °C shows a maximum at about 4 m sarcosine (Figure 6). This result has some implications of general interest, given that protein stability is very often analyzed on the basis of $\Delta_N^D G$ values at 25 °C, while what really matters for many practical purposes is the T_m value (for instance, thermostable enzymes used in recombinant DNA methodologies are useful and convenient because of their high denaturation temperatures). We have previously pointed out that, in many cases of irreversible (kinetically controlled) protein denaturation, the denaturation temperature interval has no direct relation with the denaturation Gibbs energy *versus* temperature profile (Conejero-Lara et al., 1991; Sanchez-Ruiz, 1992, 1995); in addition, the results shown in Figure 6 indicate that, *even in cases of reversible denaturation*, understanding (or enhancement) of the protein stability as conventionally measured by $\Delta_N^D G$ at 25 °C does not imply the understanding (or enhancement) of the operational stability as measured by the denaturation temperature.

The lack of correlation shown in Figure 6 is rationalized further below.

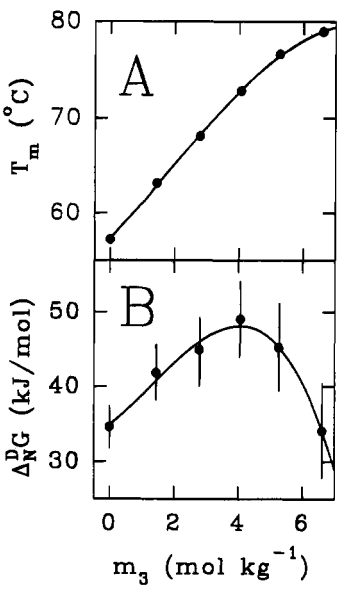

FIGURE 6: Effect of sarcosine concentration at pH° = 4.5 on RNase denaturation temperature (A) and denaturation Gibbs energy at 25 °C (B). The bars in panel B represent the standard uncertainty intervals estimated by linear propagation error, assuming that the uncertainty in the calculated $\Delta_N^D G$ arises from those of $\Delta_N^D H_m$ and $\Delta_N^D C_p$, which were taken to be 12 kJ/mol (the standard deviation of the fit of eq 13 to the denaturation enthalpy data; see Figure 3A) and 1 kJ·K^{-1}·mol^{-1} (see footnote 2 and Figure 4), respectively. In both panels, the lines represent the best fits of cubic polynomials.

Effect of Temperature and Sarcosine Concentration on the Denaturational Change in Sarcosine–Protein Preferential Interaction. From eq 7, the $\Delta_N^D \phi_{23}$ value *at the denaturation temperature* corresponding to specific pH and m_3 conditions can be calculated by using the derivative $\partial T_m/\partial m_3$ obtained from the polynomial fitting to the T_m *versus* m_3 data (see Figure 6A). Alternatively, $\Delta_N^D \phi_{23}$ values *at any temperature* may be computed as $\partial \Delta_N^D G/\partial m_3$ (eq 5) from polynomial fittings to the $\Delta_N^D G/m_3$ profiles previously derived for specific temperature and pH conditions (see, for instance, Figure 6B). As shown in Figure 7, there is an excellent agreement between the values calculated by using these two methods. [Values in Figure 7 were calculated from data at pH° = 4.5; remember, however, that under the $\Delta_N^D \nu = f$(pH) approximation, $\Delta_N^D \phi_{23}$ values do not depend on pH.]

The temperature dependencies of Figure 7 are phenomenologically related to the entropy convergence temperature and the sarcosine effect on the denaturational heat capacity change. Thus, we substitute the entropy convergence equation (eq 14, with any temperature, T, instead of T_m) into the linkage eq 8, take into account that $\Delta_N^D S^*$ has been defined as an m_3-independent parameter, and obtain:

$$\left(\frac{\partial \Delta_N^D \phi_{23}}{\partial T}\right)_{m_3} = (\partial \Delta_N^D C_p/\partial m_3) \ln (T_S^*/T) \quad (18)$$

Since $\partial \Delta_N^D C_p/\partial m_3 > 0$ (Figure 4), we have that $\partial \Delta_N^D \phi_{23}/\partial T > 0$ for $T < T_S^*$, and the denaturational change in preferential interaction increases with temperature. Furthermore, according to eq 18, the value of $\partial \Delta_N^D \phi_{23}/\partial T$ is higher, the lower the temperature and the higher the sarcosine concentration (because $\partial \Delta_N^D C_p/\partial m_3$ increases with m_3; Figure 4 and eq 15), which is precisely what we observe in Figure 7. In

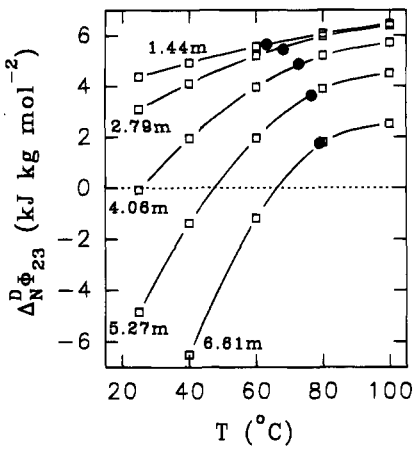

FIGURE 7: Effect of temperature and sarcosine concentration on the denaturational change in protein−sarcosine preferential interaction. This values were calculated for pH° = 4.5; however, under the $\Delta_N^D\nu = f(\text{pH})$ approximation, the $\Delta_N^D\phi_{23}$ values do not depend on pH (see text for details). (●) Values calculated from the effect of sarcosine concentration on T_m (Figure 6A and eq 7); these values are obtained at the denaturation temperatures only. (□) Values calculated from the effect of sarcosine concentration on the denaturation Gibbs energy (Figures 5 and 6B and eq 5). The lines are shown to guide the eye and have no theoretical significance.

fact, the slopes of the plots of Figure 7 show a good agreement with those calculated from eq 18 by using the T_S^* value of Table 1 and eq 15 for the m_3 dependence of $\Delta_N^DC_p$ (results not shown).

The temperature dependence of $\Delta_N^D\phi_{23}$ is particularly abrupt at the higher sarcosine concentrations (5.27 and 6.61 m, Figure 7), which merely reflects (see eq 18) the high value of $\partial\Delta_N^DC_p/\partial m_3$ at these concentrations (see eq 15 and Figure 4). As a result, for $m_3 > 4$, $\Delta_N^D\phi_{23}$ changes sign within the temperature range of Figure 7, a fact that phenomenologically rationalizes the lack of correlation between Δ_N^DG at 25 °C and denaturation temperature shown in Figure 6. Thus, $\Delta_N^D\phi_{23}$ is negative at 25 °C, $\partial\Delta_N^DG/\partial m_3 < 0$ (eq 5), and the denaturation Gibbs energy change decreases with increasing sarcosine concentration for $m_3 > 4$ m (Figure 6B). On the other hand, $\Delta_N^D\phi_{23}$ always remains positive at denaturational temperatures (Figure 7); hence, according to eq 7 and taking into account that Δ_N^DH at T_m is bound to be positive for heat denaturation, we have that $\partial T_m/\partial m_3 > 0$ and the denaturation temperature always increases with sarcosine concentration, as shown in Figure 6A.

Denaturational Change in Preferential Hydration. In principle, eq 10 allows us to calculate the denaturational change in preferential hydration, $\Delta_N^D\Gamma_{21}$, from the $\Delta_N^D\phi_{23}$ values previously determined (Figure 7). This calculation requires knowledge of the effect of cosolvent on the osmotic pressure of the water−cosolvent mixture or thermodynamically equivalent information. However, to the best of our knowledge this information is not available for water−sarcosine mixtures. Therefore, we have estimated $\Delta_N^D\Gamma_{21}$ at m_3 = 1.44 and 20 °C by using the $\partial\Pi/\partial m_3$ value [32.1 atm·kg·mol^{-1}; see Timasheff (1992)] corresponding to water−betaine mixtures at 20 °C and the betaine concentration range 0−1.5 m [note that betaine is an osmolyte with a chemical structure very similar to that of sarcosine]; this procedure yields $\Delta_N^D\Gamma_{21}$ = 71 mol of water/mol of protein for m_3 = 1.44 and 20 °C. It has been argued (Timasheff, 1992) that positive deviations of the osmotic pressure from the ideal case are one of the advantageous features of naturally occurring osmolytes. If, in spite of this consideration, we decide to insert in eq 10 the ideal $\partial\Pi/\partial m_3$ value [23.43 atm·kg·mol^{-1} for m_3 = 1.44 and 20 °C, calculated from $(RT/\bar{V}_1)/(55.56 + m_3)$], we only obtain a slightly higher value for $\Delta_N^D\Gamma_{21}$: 97 mol of water/mol of protein. If, on the other hand, we use the high $\partial\Pi/\partial m_3$ value (34.8 atm·kg·mol^{-1}) corresponding to the hypothetical superosmolyte simulated by Timasheff (1992), we arrive at $\Delta_N^D\Gamma_{21}$ = 66 mol of water/mol of protein.

Therefore, we may safely conclude that the number of extra water molecules which are thermodynamically bound to RNase upon denaturation in diluted (m_3 = 1.44) sarcosine−water is possibly around 70 and that, in any case, this number is very unlikely to be significantly higher than 100. This estimate has been calculated for T = 20 °C; nevertheless, approximately the same value should hold for other temperatures, since $\partial\Pi/\partial m_3$ and $\Delta_N^D\phi_{23}$ (Figure 7) do not depend much on temperature at m_3 = 1.44.

The following two lines of reasoning show that $\Delta_N^D\Gamma_{21} \approx$ 70 mol of water/mol of protein is much smaller than what could be intuitively expected from some common assumptions:

(1) Seventy is of the same order as the osmotic stress estimates of the number of water molecules implicated in some ligand-binding processes. For instance, about 60 extra water molecules appear to bind to hemoglobin upon full oxygenation (Colombo et al., 1992) and about 100 appear to be released upon binding of glucose to hexokinase (Rand & Fuller, 1992). This qualitative agreement between the number of water molecules implicated in denaturation and ligand-binding processes is surprising, especially if one expects this number to reflect the magnitude of the conformational changes involved.

(2) Osmolytes, such as sarcosine, are strongly excluded from the surface of the native protein (Arakawa & Timasheff, 1985; Timasheff, 1992) and the concomitant preferential hydration may be modeled (at least as a rough, first approximation) by a layer of water with a sharp boundary between it and the bulk solvent (Timasheff, 1992). Density measurements (Lee et al., 1979) indicate that, in most cases, this preferential hydration of the native protein is in the range of 0.4−0.6 g of water/g of protein (for instance, for lysozyme in water−sarcosine it is 0.48 g/g; Arakawa & Timasheff, 1985); this range appears to be only slightly larger than some estimates of the hydration required to achieve monolayer coverage [for instance, 0.38 g/g for lysozyme from studies into the effect of hydration on the protein heat capacity (Yang & Rupley, 1979) or 0.34 g/g from measurements of the nonfreezing water (Kuntz, 1971); for a review on these and other methods see Gregory (1995)]. If we conservatively assume that a value of 0.4 g/g is valid for RNase in sarcosine−water, we have that about 300 water molecules preferentially hydrate the native protein; that is, $\Gamma_{21}^N \approx$ 300 mol of water/mol of protein. Now, preferential exclusion of osmolytes is thought to be due to nonspecific mechanisms, such as the increase in water surface tension, which are independent of the nature of the protein surface (Timasheff, 1992) and, hence, simply proportional to the total area exposed to the solvent. The water-accessible surface area for native RNase is 6790 Å^2, while that for denatured RNase

would be 20 200 Å^2 if the denatured state is assumed to be a fully solvated chain [both values taken from Miller et al. (1987)]. According to these ASA values, the preferential hydration of the denatured RNase should be about 3 times larger than that for the native protein: $\Gamma_{21}^D \approx 900$ mol of water/mol of protein[3] and the denaturational change in preferential hydration is predicted to be $\Delta_N^D\Gamma_{21} = \Gamma_{21}^D - \Gamma_{21}^N \approx 600$ mol of water/mol of protein, which is about 1 order of magnitude larger than 70.[4]

Clearly, some explanation is required for the surprisingly low $\Delta_N^D\Gamma_{21}$ value (about 70 mol of water/mol of protein) calculated from experimental data. In fact, two possible explanations (A and B) are offered below:

(A) Sarcosine is strongly excluded from the surface of both the native and denatured RNase, but the denatured state is not a fully solvated chain (therefore, its ASA is much smaller than 20 000 Å^2). This would be consistent with recent studies which suggest that thermally denatured RNase retains significant structure (Sosnick & Trewhella, 1992; Seshadri et al., 1994). On the other hand, this possibility would appear to be disfavored by the fact that the experimental value for denaturational heat capacity change for RNase (and other globular proteins) agrees with that predicted by eq 16 (or equivalent approaches), together with the $\Delta_N^D ASA_{pol}$ and $\Delta_N^D ASA_{ap}$ values calculated assuming a fully solvated denatured state (Murphy & Gill, 1991; Spolar et al., 1992; Privalov & Makhatadze, 1992; Yang et al., 1992; Murphy & Freire, 1992; Murphy et al., 1992; Sanchez-Ruiz, 1995; Makhatadze & Privalov, 1995). We must remember, however, that the polar and apolar contributions in eq 16 *have different signs*; hence, it is mathematically possible to reproduce the experimental $\Delta_N^D C_p$ value by using values for the polar and apolar ASA smaller than those calculated by assuming a fully solvated denatured state.

(B) In diluted aqueous solutions of sarcosine, denatured RNase does behave as a fully-solvated chain, but sarcosine is not strongly excluded from the surface of the denatured state (that is, the denatured state is fully solvated, but by water *and sarcosine*). Of course, this requires that new specific interactions between sarcosine and the protein be created upon denaturation.[5] In fact, this type of situation would have some precedents; thus, cosolvents like poly(ethylene glycol) (Lee & Lee, 1987) and 2-methyl-2,4-pentanediol (Pittz & Timasheff, 1978) are thought to be preferentially excluded from the surface of native proteins and, at the same time, to interact favorably with denatured proteins.

We cannot decide between these two possibilities (A and B), or a combination of both, on the basis of the data presented in this paper only. We note, nevertheless, that both cases have interesting implications. Thus, if explanation A is true, then studies into the effect of osmolytes (such as sarcosine) on protein stability could be used to quantify the degree of hydration of denatured proteins, thus providing an independent measure of the consequences of the possible residual structure. If, on the other hand, explanation B is true, then it would be possible, at least in principle, to find (or, perhaps, design) substances that are more efficient protein stabilizers than sarcosine or other osmolytes are. This is easily shown by the following "back-of-the-envelope" calculation. Assume that denatured RNase behaves as a fully solvated chain and that a certain substance is strongly excluded from the surface of both the native and the denatured protein; then, for RNase denaturation in diluted aqueous solutions of this substance (cosolvent) we should expect $\Delta_N^D\Gamma_{21} \approx 600$ mol of water/mol of protein. Now, using a typical value for $\partial\Pi/\partial m_3$ (30 atm·kg·mol^{-1}, for instance) and eq 10, we arrive at a denaturational change in cosolvent−protein preferential interaction ($\Delta_N^D\phi_{23}$) of about 33 kJ·kg·mol^{-2}. Finally, this latter value may be used in eq 7, together with typical values of $\Delta_N^D H_m$ and T_m (for instance, $\Delta_N^D H_m = 443$ kJ/mol and $T_m = 330$ K, which are for RNase denaturation in water, pH = 4.5) to find the following estimate of the effect of cosolvent concentration on denaturation temperature: $\partial T_m/\partial m_3 \approx 25$ K·mol^{-1}·kg, which is about 5 times larger than the experimental values found for sarcosine (Figure 6A) and other osmolytes (Arakawa & Timasheff, 1985; Santoro et al., 1992). Therefore, even a comparatively low concentration of this hypothetical substance would cause a very large increment in denaturation temperature.

The above considerations suggest the interest of systematically applying the methodology employed in the present paper to the study of the effect of several cosolvents on the thermodynamic stability of model proteins. Suppose, for instance, that, under certain conditions, the hydration of both the native and denatured state of a given protein may be represented as a layer of water which is impenetrable to, at least, certain kinds of substances; then we should be able to find several, chemically different cosolvents that yield approximately the same value for $\Delta_N^D\Gamma_{21}$, a result which would support that situation A holds for these cosolvents. In fact, the approach based on the use of several cosolvents of different chemical nature has been recently employed, combined with the osmotic stress method, to determine the number of water molecules taken from the solvent upon full oxygenation of hemoglobin (Colombo et al., 1992). The theoretical and experimental approaches presented in this paper suggest that the same approach may be feasible and useful in the analysis of protein folding and stability. Work along this line has already begun in this laboratory.

ACKNOWLEDGMENT

We thank Drs. G. Makhatadze and P. Privalov for providing copies of manuscripts prior to publication.

[3] Using a similar argument, Gregory (1995) concludes that about 360−400 molecules of water are required to hydrate native lysozyme and about 1000−1400 to hydrate the denatured state, if this is assumed to be a fully solvated chain.

[4] The ASA value for the fully solvated denatured state (about 20 000 Å^2) we have used in our calculations is that given by the sum of the ASA of the constituent residues in an extended Gly-X-Gly peptide (Miller et al., 1987). Values about 15% smaller are obtained by modeling the denatured state as an extended β-chain (Livingstone et al., 1991). Using this latter ASA values, our predicted $\Delta_N^D\Gamma_{21}$ would be about 450 mol of water/mol of protein, still more than 6 times the value (70) estimated from the experimental DSC data.

[5] For instance, the apolar parts of the osmolyte might interact favorably with the hydrophobic side chains which are exposed upon denaturation; this interesting possibility was put forward by Santoro et al. [1992; see also see Arakawa and Timasheff (1983)] in order to rationalize the effect of the degree of methylation on the T_m increase caused by glycine-based osmolytes. We note, however, that this interaction would be intuitively expected to lower the denaturation heat capacity (upon interaction, some apolar ASA in the denatured state would be removed from contact with water), while the overall effect we observe (Figure 4) is an increase in $\Delta_N^D C_p$ with sarcosine concentration.

SUPPORTING INFORMATION AVAILABLE

Mathematical derivations for some of the equations given in the Basic Theory section and additional details regarding the linkage between temperature, cosolvent, and pH effects on denaturation thermodynamics (7 pages). Ordering information is given on any current masthead page.

REFERENCES

Alberty, R. A. (1969) *J. Am. Chem. Soc. 91*, 3899−3903.
Arakawa, T., & Timasheff, S. N. (1983) *Arch. Biochem. Biophys. 224*, 169−177.
Arakawa, T., & Timasheff, S. N. (1985) *Biophys. J. 47*, 411−414.
Baldwin, R. L., & Muller, N. (1992) *Proc. Natl. Acad. Sci. U.S.A. 89*, 7110−7113.
Becktel, W. J., & Schellman, J. A. (1987) *Biopolymers 26*, 1859−1877.
Bevington, P. R. (1969) *Data Reduction and Error Analysis of the Physical Sciences*, McGraw-Hill, New York.
Blinder, S. M. (1966) *J. Chem. Educ. 43*, 85−92.
Brandts, J. F., & Lin, L.-N. (1990) *Biochemistry 29*, 6927−6940.
Christensen, J. J., Hansen, L. D., & Izatt, R. M. (1976) *Handbook of Proton Ionization Heats*, Wiley, New York.
Colombo, M. F., Rau, D. C., & Parsegian, V. A. (1992) *Science 256*, 655−659.
Conejero-Lara, F., Mateo, P. L., Avilés, F. X., & Sanchez-Ruiz, J. M. (1991) *Biochemistry 30*, 2067−2072.
Doig, A. J., & Williams, D. H. (1992) *Biochemistry 31*, 9371−9375.
Fu, L., & Freire, E. (1992) *Proc. Natl. Acad. Sci. U.S.A. 89*, 9335−9338.
Galisteo, M. L., Mateo, P. L., & Sanchez-Ruiz, J. M. (1991) *Biochemistry 30*, 2061−2066.
Gregory, R. B. (1995) in *Protein−Solvent Interactions* (Gregory, R. B., Ed.) pp 191−264, Marcel Dekker, New York.
Kuntz, I. D. (1971) *J. Am. Chem. Soc. 93*, 514−516.
Lee, B. (1991) *Proc. Natl. Acad. Sci. U.S.A. 88*, 5154−5158.
Lee, J. C., & Lee, L. L. Y. (1987) *Biochemistry 26*, 7813−7819.
Lee, J. C., Gekko, K., & Timasheff, S. N. (1979) *Methods Enzymol. 61*, 26−49.
Livingstone, J. R., Spolar, R. S., & Record, M. T. (1991) *Biochemistry 30*, 4237−4244.
Makhatadze, G. I., & Privalov, P. L. (1990) *J. Mol. Biol. 213*, 375−384.
Makhatadze, G. I., & Privalov, P. L. (1993) *J. Mol. Biol. 232*, 639−659.
Makhatadze, G. I., & Privalov, P. L. (1995) *Adv. Protein Chem.* (in press).
Miller, S., Janin, J., Lesk, A. M., & Chothia, C. (1987) *J. Mol. Biol. 196*, 641−656.
Murphy, K. P., & Gill, S. J. (1990) *Thermochim. Acta 172*, 11−20.
Murphy, K. P., & Gill, S. J. (1991) *J. Mol. Biol. 222*, 699−709.
Murphy, K. P., & Freire, E. (1992) *Adv. Protein Chem. 43*, 313−361.
Murphy, K. P., Privalov, P. L., & Gill, S. J. (1990) *Science 247*, 559−561.
Murphy, K. P. Bhakuni, V., Xie, D., & Freire, E. (1992) *J. Mol. Biol. 227*, 293−306.
Pittz, E. P., & Timasheff, S. N. (1978) *Biochemistry 17*, 615−623.
Privalov, P. L. (1979) *Adv. Protein Chem. 33*, 167−241.
Privalov, P. L. (1989) *Annu. Rev. Biophys. Biophys. Chem. 18*, 47−69.
Privalov, P. L., & Khechinashvili, N. N. (1974) *J. Mol. Biol. 86*, 665−684.
Privalov, P. L., & Gill, S. J. (1988) *Adv. Protein Chem. 39*, 191−234.
Privalov, P. L., & Makhatadze, G. I. (1990) *J. Mol. Biol. 213*, 385−391.
Privalov, P. L., & Makhatadze, G. I. (1992) *J. Mol. Biol. 224*, 715−723.
Privalov, P. L., & Makhatadze, G. I. (1993) *J. Mol. Biol. 232*, 660−679.
Privalov, P. L., Plotnikov, V. V., & Filimonov, V. V. (1975) *J. Chem. Thermodyn. 7*, 41−47.
Privalov, P. L., Tiktopulo, E. I., Venyamov, S. Y., Griko, Y. V., Makhatadze, G. I., & Khechinashvili, N. N. (1989) *J. Mol. Biol. 205*, 737−750.
Rand, R. P., & Fuller, (1992) *Biophys. J. 61*, A345.
Sanchez-Ruiz, J. M. (1992) *Biophys. J. 61*, 921−935.
Sanchez-Ruiz, J. M. (1995) in *Subcellular Biochemistry, Volume 24: Proteins: Structure, Function and Engineering* (Biswas, B. B., & Roy, S., Eds.) pp 133−176, Plenum, New York.
Santoro, M. M., Liu, Y., Khan, S. M. A., Hou, L.-X., & Bolen, D. W. (1992) *Biochemistry 31*, 5278−5283.
Scatchard, G. (1946) *J. Am. Chem. Soc. 68*, 2315−2319.
Seshadri, S., Oberg, K. A., & Fink, A. L. (1994) *Biochemistry 33*, 1351−1355.
Sosnick, T. R., & Trewhella, J. (1992) *Biochemistry 31*, 8329−8335.
Spolar, R. S., Livingstone, J. R., & Record, M. T. (1992) *Biochemistry 31*, 3947−3955.
Timasheff, S. N. (1992) in *Water and Life* (Somero et al., Eds.) pp 70−84, Springer-Verlag, Berlin.
Timasheff, S. N. (1993) *Annu. Rev. Biophys. Biomol. Struct. 22*, 67−97.
Wyman, J. (1964) *Adv. Protein Chem. 19*, 223−286.
Yancey, P. H., Clark, M. E., Hand, S. C., Bowlus, R. D., & Somero, G. N. (1982) *Science 217*, 1214−1222.
Yang, A.-S., Sharp, K. A., & Honig, B. (1992) *J. Mol. Biol. 227*, 889−900.
Yang, P., & Rupley, J. A. (1979) *Biochemistry 18*, 2654−2661.

BI950352W